PLASMA, HYDRO- AND GAS DYNAMICS

On the Formation of a Plasma Cloud at the Ablation of a Pellet in a High-Temperature Magnetized Toroidal Plasma

O. A. Bakhareva[a, *], V. Yu. Sergeev[a], and I. A. Sharov[a]

[a] *Peter the Great St. Petersburg Polytechnic University, St. Petersburg, 195251 Russia*

*e-mail: o.bakhareva@spbstu.ru

The investigation of cold secondary plasma clouds near pellets ablating in the hot plasma of magnetic confinement devices (tokamaks and stellarators) provides valuable information on the physical characteristics of a pellet cloud. In this work, the characteristic sizes of emitting clouds around fusible polystyrene pellets and refractory carbon pellets have been analyzed. The calculation of the ionization length of C^+ ions in both carbon and hydrocarbon clouds has shown that the contribution of only hot electrons is insufficient to ensure the experimentally observed decay lengths of the CII line intensity. Taking into account the strong shielding of the electron flux of the background plasma in the hydrocarbon pellet cloud, the ionization of C^+ ions in this cloud is determined predominantly by electrons of the cold plasma of the cloud. Shielding near a refractory carbon pellet is weak because its ablation rate is lower. The contributions from hot electrons of the surrounding plasma and cold electrons of the pellet cloud to the ionization of C^+ ions are comparable in the case of carbon pellets.

1. INTRODUCTION

The injection of macroparticles (pellets) of various materials such as H_2, D_2, Li, C, and C_8H_8 into the plasma of magnetic confinement devices is widely used to control the parameters of a discharge and its diagnostic [1, 2]. Information on the spatial distribution of atoms and ions in different charged states in a cloud is necessary to compare factors of neutral and plasma shielding of heat fluxes reaching the pellet surface [3] and to refine the efficiency of pellet surface ions of the plasma in the pellet cloud owing to their recombination and charge-exchange [4].

Longitudinal and transverse (with respect to the local magnetic field) distributions of the CII (723 nm) line intensity of C^+ ions were previously analyzed for clouds near ablating carbon and hydrocarbon pellets. It was observed in [5] that the characteristic longitudinal decay length of the CII line intensity l_{dec} in carbon clouds at the Wendelstein 7-AS (W7-AS) approximately corresponds to the ionization length of C^+ ions by hot electrons of the background plasma evaluated by the expression

$$l_{ion}^{hot} = \frac{u}{n_e \langle \sigma_{C^+ \to 2+} v \rangle_{T_e}}. \qquad (1)$$

Here, u is the velocity of longitudinal expansion of the ablatant, which is equated to the speed of sound $c_s = \sqrt{\dfrac{5}{3}\dfrac{T_{cld}}{m_C}}$, where $T_{cld} = 1.0$ eV is the electron temperature in the cloud and m_C is the mass of the C atom; n_e is the background plasma density; and $\langle \sigma_{C^+ \to 2+} v \rangle_{T_e}$ is the rate coefficient of electron-impact ionization of the C^+ ion calculated with the Maxwell distribution function with the temperature of hot electrons T_e [6]. At the same time, the simulation of the parameters of carbon pellet clouds at the W7-AS using the LLP numerical code [7] gives higher electron temperatures in the cloud of 2.5−5 eV. The rate coefficient of electron-impact ionization of the C^+ ion $\langle \sigma_{C^+ \to 2+} v \rangle_{T_{cld}}$ at low temperatures of 1−4 eV decreases by more than an order of magnitude when T_{cld} decreases by 1 eV [6]. For this reason, $\langle \sigma_{C^+ \to 2+} v \rangle_{T_{cld}=1\,eV} \ll \langle \sigma_{C^+ \to 2+} v \rangle_{T_e}$ was accepted in [5] at $T_{cld} = 1.0$ eV and it was assumed that only hot electrons of the background plasma make the leading contribution to the ionization of C^+ ions. The contribution of the electrons of the cloud to ionization at temperatures of the secondary cold plasma of 2.5−5 eV should be noticeably larger; therefore, conclusions made in [5] should be refined.

In experiments at the Large Helical Device (LHD), the electron density $n_{cld} \cong 4 \times 10^{16} - 2 \times$

10^{17} cm^{-3} [8] and the electron temperature $T_{\text{cld}} \cong 2$–6 eV [9] were measured and the characteristic dimensions of emitting regions of hydrocarbon clouds were studied [10], in particular, at the CII (723 nm) line. The main results of the measurement and interpretation of dimensions of clouds were obtained under the assumption that cold electrons of a cloud itself make the decisive contribution to ionization. The contribution of hot electrons was not estimated explicitly.

The aim of this work is to analyze the parameters of the secondary cold plasma near carbon and hydrocarbon pellets ablated in the W7-AS and LHD plasmas in order to compare the contributions of cold electrons of the cloud and hot electrons of the background plasma to the ionization of C$^+$ ions in pellet clouds.

2. HOT-ELECTRON IONIZATION OF C$^+$ IONS IN THE CLOUD

When the effective decrease in the density of hot electrons of the background plasma by a factor of $\delta_{n,\text{plc}}$ after their passage through the plasma cloud is taken into account, expression (1) for the characteristic ionization length of the C$^+$ ion is transformed to

$$l_{\text{ion}}^{\text{hot}} = \frac{u}{\delta_{n,\text{plc}} n_e \langle \sigma_{\text{C}^+ \to 2+} v \rangle}. \qquad (2)$$

To estimate the shielding factor of the electron density by the pellet plasma cloud $\delta_{n,\text{plc}}$, we used the shielding factor for the heat flux δ_q, which was determined from experimental data using the energy balance on the pellet surface:

$$\delta_q = \frac{\varepsilon \dot{N}}{q_e 2\pi r_\text{p}^2}. \qquad (3)$$

Here, r_p is the current pellet radius; ε is the effective sublimation energy ($\varepsilon \cong 8.8$ eV for the C atom [11] and $\varepsilon \cong 1.5$ eV for the C$_8$H$_8$ polystyrene monomer [12]); $q_e = \frac{1}{4} n_e \sqrt{\frac{8T_e}{\pi m_e}} \times 2T_e$ is the unperturbed heat flux density carried by hot electrons; $\dot{N}$ is the pellet ablation rate; n_e and T_e are the electron density and temperature in the surrounding plasma, respectively; and m_e is the mass of the electron.

To determine the relation between $\delta_{n,\text{plc}}$ and δ_q, we make several assumptions. First, we assume that the shielding factor for the heat flux of electrons of shielding factor for the product of the shielding factors in the neutral and plasma parts of the cloud $\delta_q = \delta_{q,nc} \delta_{q,\text{plc}}$. The same relation $\delta_n = \delta_{n,nc} \delta_{n,\text{plc}}$ is assumed for the suppression of hot electron flux. Second, we assume that the shielding factors of the hot electron flux and hot electron heat flux are slightly different, i.e., $\delta_{q,nc} \cong \delta_{n,nc}$ and $\delta_{q,\text{plc}} \cong \delta_{n,\text{plc}}$. This

assumption is based on the analysis of the joint solution of the kinetic equation and the energy loss equation for electrons of the background plasma in the neutral pellet cloud [13]. It is valid for both refractory carbon and fusible hydrocarbon (polystyrene) pellets, although the typical factors of neutral shielding for carbon, $\delta_{q,nc} \cong 0.8$, and hydrocarbon, $\delta_{q,nc} \cong 0.02$, clouds are strongly different. We note that the author of [14], analyzing the neutral shielding for the case of hydrogen pellet ablation, also concluded that $\delta_{n,nc}$ and $\delta_{q,nc}$ are comparable. Third, it is assumed that the shielding factors in the neutral and plasma parts of the pellet cloud are comparable: $\delta_{q,nc} \cong \delta_{q,\text{plc}}$ and $\delta_{n,nc} \cong \delta_{n,\text{plc}}$. This follows from estimates of the integral thicknesses of the neutral and plasma parts of hydrocarbon clouds from data reported in [8, 9] and is consistent with conclusions made in [15], where the effect of neutral and plasma clouds on the carbon pellet ablation rate was evaluated.

Under the listed assumptions, we obtain $\delta_q = \delta_{q,nc} \delta_{q,\text{plc}} = \delta_{n,nc} \delta_{n,\text{plc}} = \delta_{n,\text{plc}}^2$ and, thereby,

$$\delta_{n,\text{plc}} = \sqrt{\delta_q}. \qquad (4)$$

In experiments at the W7-AS [5], carbon pellets 0.35–0.45 mm in diameter were injected into the plasma at a velocity of 150–400 m/s in the direction of the magnetic axis of the plasma column. The radiation of carbon pellet clouds was detected using an optical system at an angle of about 46° in the poloidal direction to the axis of injection. The exposure time of a CCD camera was varied in a wide range from 1 μs to 10 ms, which allowed us to obtain both series of one to ten photographs of the pellet cloud and integral photographs of the cloud, which were formed by the moving glowing pellet cloud during the pellet ablation process. The CII line radiation was detected using a 720 nm filter with a FWHM of the passband of 9.3 nm or a 723 nm filter with a FWHM of 1.9 nm. The experiments and results were described in more detail in [16].
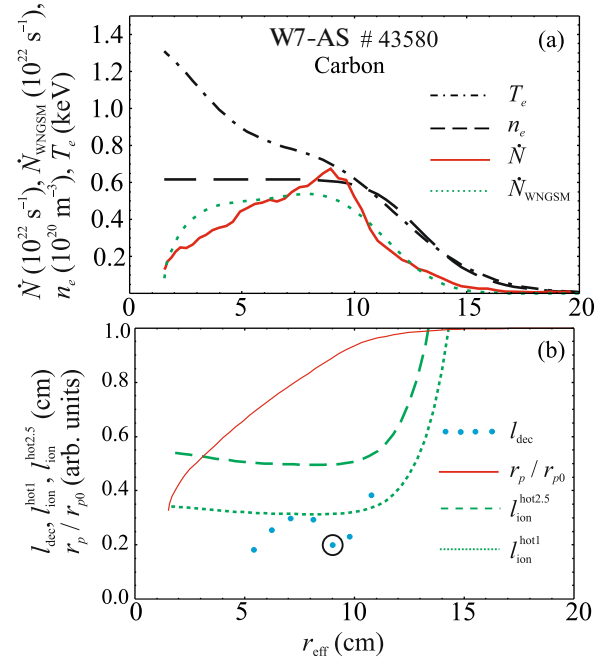
The distribution of the CII line intensity of the carbon pellet cloud along the longitudinal axis of the cloud corresponding the position of the pellet at an effective minor radius of $r_{\text{eff}} \approx 9$ cm for discharge no. 43580 is shown by the dotted line in Fig. 1. The discharge at the injection time had the parameters $n_{e0} = 6.2 \times 10^{13}$ cm^{-3}, $T_{e0} = 1.4$ keV, $P_{\text{ECRH}} = 410$ kW, $R_0 = 2.05$ m, $a_{\text{eff}} = 0.17$ m, and $B = 2.55$ T, and the pellet had the initial radius $r_{\text{p0}} = 0.19$ mm and velocity $v_\text{p} = 310$ m/s [5]. The local electron temperature and density in the background plasma and the current pellet radius at $r_{\text{eff}} \approx 9$ cm were $T_e = 0.7$ keV, $n_e = 6.07 \times 10^{13}$ cm^{-3}, and $r_\text{p} = 0.18$ mm, respectively. The red solid lines in Fig. 1 show rms fitted exponen-
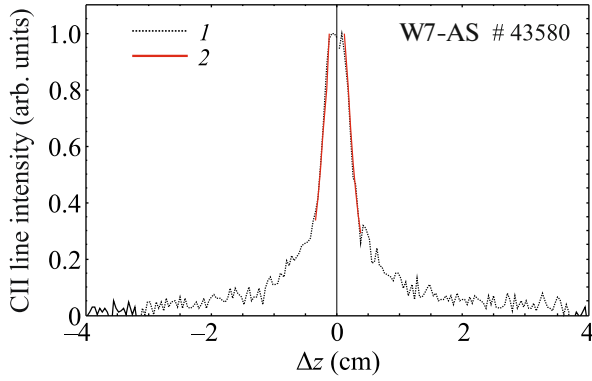
Fig. 1. (Color online) Distribution of the CII (723 nm) line intensity in the cloud along the magnetic field on the instantaneous photograph in discharge no. 43580 at the W7-AS at $r_{eff} \approx 9$ cm: (*1*) intensity distribution along the longitudinal axis of the cloud and (*2*) fitted exponential dependences in the region of the rapid decrease in the intensity.

Fig. 2. (Color online) Parameters of the background plasma and pellet ablation versus its spatial position on the path in the outer part of the plasma column.

tial dependences with the characteristic length l_{dec} where the intensity decreases by a factor of e. The l_{dec} values are close on the right and left wings of the longitudinal distribution of the CII line intensity with respect to the position of the pellet $\Delta z = 0$ cm. Below, we use the average value for two wings. The average value for the distribution presented in Fig. 1 is $l_{dec} = 2$ mm.

Figure 2 shows the dependences of the pellet ablation rate $\dot{N}$, the ratio of its radius to the initial value r_p/r_{p0}, the electron density n_e and temperature T_e in the background plasma, the characteristic longitudinal decay lengths l_{dec} in the CII line intensity, and the lengths of the electron impact ionization of C^+ ions l_{ion}^{hot1} and $l_{ion}^{hot2.5}$ calculated by Eq. (2) at two longitudinal expansion rates of the secondary cold plasma of the pellet cloud for discharge no. 43580 W7-AS on the effective minor radius of the magnetic surface r_{eff}. The length l_{ion}^{hot1} was calculated under the assumption that $u = c_s$ at an electron temperature of $T_{cld} = 1$ eV in the cloud as in [5], and the length $l_{ion}^{hot2.5}$ was calculated for $u = c_s$ at $T_{cld} = 2.5$ eV, which corresponds to the lower bound of the calculated temperature of the carbon cloud from [7]. The shielding factor δ_q was in the range from 0.7 to 1, and the ionization lengths were calculated with the average value $\delta_{n,plc} \approx 0.9$, which insignificantly affects the calculated ionization lengths. The pellet ablation rate $\dot{N}_{WNGSM}$ was calculated within the weak neutral shielding model [11]. The circle in Fig. 2 marks the l_{dec} value found for the longitudinal distribution in Fig. 1.

The comparison of l_{dec} values at $r_{eff} = 5-11$ cm shows that the characteristic longitudinal decay length of the CII line intensity l_{dec} deceases generally as the pellet approaches the center of the plasma column. Two l_{dec} values at $r_{eff} = 9$ and 10 cm that are smaller than those at the neighboring points are in the region where the pellet is ablated more rapidly than one could expect under the assumption of the Maxwell distribution of particles in the background plasma, which corresponds to the local n_e and T_e values. Suprathermal particles were probably present in the region $r_{eff} = 9-10$ cm in discharge no. 43580 and could have increased the ablation rate and enhanced the ionization of C^+ ions in the cloud compared to the case of the Maxwellian background plasma. As the pellet further approaches the center of the plasma column in the region of the hotter and denser background plasma at $r_{eff} \leq 8$ cm, the characteristic decay length l_{dec} continues to decrease and the dimension of the pellet, as well as the number of ablated atoms at the final stage of ablation, decreases noticeably. With a decrease in r_{eff}, the calculated ionization lengths l_{ion}^{hot1} and $l_{ion}^{hot2.5}$ first decrease apparently because of an increase in the density of the background plasma n_e and then increase slightly because n_e already hardly changes, and the ionization cross section decreases slightly with an increase in the temperature T_e of hot electrons.

The comparison of the characteristic decay lengths l_{dec} with the ionization lengths in Fig. 2b indicates that
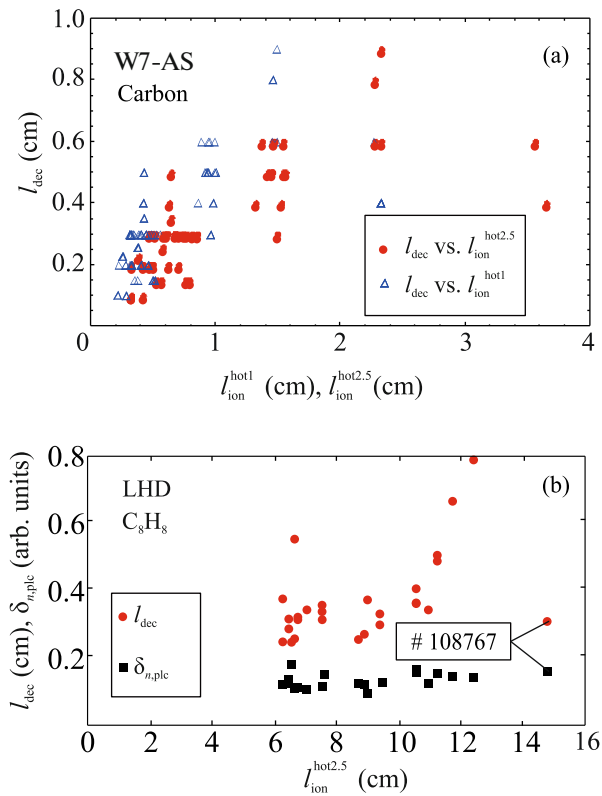
Fig. 3. (Color online) Observed longitudinal length of the CII line intensity l_{dec} versus the ionization length l_{ion}^{hot} (a) for carbon clouds at the W7-AS (the l_{ion}^{hot1} and $l_{ion}^{hot2.5}$ values are given on the horizontal axis) and (b) for hydrocarbon clouds at the LHD (the calculated $\delta_{n,plc}$ values used to calculate $l_{ion}^{hot2.5}$ are also presented).

ionization induced by hot background plasma electrons at the expansion of the cloud at the speed of sound corresponding to $T_{cld} = 1$ eV assumed in [5] can sometimes be enough to explain the observed decay lengths of the CII line intensity. However, the contribution of only hot electrons is insufficient at $T_{cld} = 2.5$ eV.

The characteristic lengths of the cloud l_{dec} measured at the times of the most intense ablation of carbon pellets for various discharges at the W7-AS are shown in Fig. 3a in comparison with the calculated ionization lengths l_{ion}^{hot1} and $l_{ion}^{hot2.5}$. The cloud shielding of hot background plasma electrons was insignificant in these experiments, and the l_{ion}^{hot1} and $l_{ion}^{hot2.5}$ values shown in Fig. 3a were calculated with $\delta_{n,plc} \cong 0.9$. The electron density and temperature of the background plasma in the center of the plasma column in the discussed experiments were in the ranges of $n_{e0} = (1-10) \times 10^{19}$ m^{-3} and $T_{e0} = 0.5-6.0$ keV, respectively. As seen in Fig. 3a, under the assumption of the longi-

tudinal expansion of the cloud at the speed of sound corresponding to the temperature $T_{cld} = 1$ eV, the characteristic longitudinal decay lengths of the CII line intensity are comparable with the length of hot-electron ionization of C$^+$ ions, as mentioned in [5]. However, this agreement between the measured and calculated characteristic lengths is worsened at a more realistic temperature of the carbon cloud of $T_{cld} = 2.5$ eV.

In experiments at the LHD heliotron, polystyrene pellets 0.9 mm in diameter were injected into the plasma in the equatorial plane at velocities of 400–500 m/s. Images of the emitting cloud in nine spectral ranges determined by the set of interference filters were obtained once per discharge using an imaging polychromator [8]. To detect the CII line radiation from the pellet cloud, one of the channels of the polychromator was equipped with a 724.5 nm filter with a FWHM of 4.5 nm. The angle between the polychromator observation direction and the injection axis was about 2°. Recording with an exposure time of 10–30 μs along the trajectory provided instantaneous photographs of the pellet cloud. In addition, data from the polychromator allowed the determination of the spatial distributions of the electron density [8] and temperature [9] in the hydrocarbon cloud from the broadening of the H$_\beta$ line of hydrogen emission and from the ratio of the local emission coefficients of the H$_\beta$ line and the continuous spectrum.

The measured characteristic longitudinal decay lengths l_{dec} of the CII line intensity in hydrocarbon clouds at the LHD are shown in Fig. 3b in comparison with the lengths of electron-impact ionization of C$^+$ ions $l_{ion}^{hot2.5}$ calculated by Eq. (2). The velocity of longitudinal expansion was taken the speed of sound $u = c_s$ corresponding to the measured temperature of the hydrocarbon cloud $T_{cld} = 2.5$ eV [9]. The shielding factor $\delta_{n,plc}$ was calculated from experimental data as described above by Eqs. (3) and (4). The presented data were obtained for a set of discharges at electron densities of $(1-7) \times 10^{19}$ m^{-3} and electron temperatures of $0.5-1.5$ keV in the background plasma.

Table 1 presents l_{dec} and $\delta_{n,plc}$ values for discharge no. 108767 measured at the time when the pellet was located in the LHD at an effective minor radius of $r_{eff} \approx 39$ cm. During the hydrocarbon pellet ablation at LHD, $\delta_{n,plc}$ is noticeably smaller than 1 and, correspondingly, l_{ion}^{hot} values calculated by Eq. (2) are much larger than the measured l_{dec} values. The results confirm the assumption made in [10] that cold electrons of the cloud itself make decisive contribution to the ionization balance of C$^+$ ions.

3. HOT AND COLD ELECTRON IONIZATION OF C⁺ IONS IN THE CLOUD

An expression for the calculation of ionization lengths including the contributions from both hot and cold electrons is more general than Eqs. (1) and (2) and has the form

$$l_{ion}^{total} = \frac{M_{cdl} c_s}{\delta_{n,pcl} n_e \langle \sigma_{C^+ \to 2+} v \rangle + n_{cld} \langle \sigma_{C^+ \to 2+} v \rangle_{T_{cld}}}. \quad (5)$$

Here, $\langle \sigma_{C^+ \to 2+} v \rangle_{T_{cld}}$ is the rate coefficient of electron-impact ionization of the C^+ ion to the C^{2+} ion calculated with the Maxwell distribution function with the temperature of cold electrons [6], and $M_{cld} = u/c_s$ is the Mach number in the cloud, which above is taken to be 1. When evaluating the contribution of hot electrons to the ionization rate, it was taken into account that the plasma part of the cloud reduces the electron flux by a factor of $\delta_{n,plc}$, as described in Section 2.

We used the simplest estimate for the density of heavy particles from the condition of material balance

$$2\pi r_{cld}^2 n_{hvy} u = \dot{N}, \quad (6)$$

where n_{hvy} is the total density of ions in all charge states averaged over the cross section of the cloud and r_{cld} is the transverse radius of the cloud. In the region of intense ionization of C^+ ions, it is assumed that all atoms are singly ionized; consequently, the densities of electrons and heavy particles are the same: $n_{cld} = n_{hvy}$. The electron and ion temperatures were taken the same because the frequencies of electron–electron and electron–ion collisions in the dense plasma of pellet clouds are about $10^{11}–10^{12}$ s⁻¹ and $10^6–10^7$ s⁻¹, respectively, which exceeds the possible inverse time of variation of the plasma parameters in the cloud that can be estimated as $u/l_{dec} \sim 10^6$ s⁻¹. The radius of the expansion channel r_{cld} was estimated in experiments as the HWHM of the transverse distribution of the CII line intensity. This estimate should be treated as an upper estimate because even a small degree of ionization of the ablatant is sufficient to completely stop its convective expansion across the magnetic field [17], and the beginning of secondary ionization guarantees the localization of the material in the channel with such radius.

The electron density and temperature in the hydrocarbon pellet cloud at the LHD were measured directly in the experiment in a small part of the cloud where H_β line emission was observed. The electron density and densities of ions in various charge states in carbon clouds were calculated [7]. All these data were used to verify the conservation law given by Eq. (6).

Data for discharge no. 108767 summarized in Table 1 were used for the polystyrene pellet ablation in the plasma of the LHD heliotron. The image of the cloud was obtained when the pellet was at an effective

Table 1. Parameters of the pellet and the surrounding plasma and the transverse dimension of the emitting region near the pellet in discharges no. 43580 W7-AS (when the pellet is at $r_{eff} \approx 9$ cm) and no. 108767 LHD (when the pellet is at $r_{eff} \approx 39$ cm)

Parameter\discharge	W7-AS no. 43580	LHD no. 108767
$P_{ECRH+NBI}$ (MW)	0.45	9.9
r_p (mm)	0.18	0.33
v_p (m/s)	310	483
r_{eff} (m)	0.09	0.39
n_e (10^{19} m⁻³)	6.07	1.96
T_e (keV)	0.70	1.37
$\dot{N}$ (10^{21} s⁻¹)	6.7	2.84*
δ_q	0.81	0.019
$\delta_{n,plc}$	0.9	0.14
l_{dec} (mm)	2.0	2.9
$l_{ion}^{hot1}; l_{ion}^{hot2.5}$ (mm)	3.1; 4.9	97; 153
r_{cld} (mm)	2.7	3.0

*In C_8H_8 monomers.

minor radius of $r_{eff} \approx 39$ cm, and the measured ablation rate was $\dot{N} \cong 2.8 \times 10^{21}$ s⁻¹ (in C_8H_8 monomers). The electron temperature and density at a distance of $\Delta z \cong 5.8$ mm from the center of the cloud, where the intense ionization of C^+ ions began, were $T_{cld} = 3.3$ eV and $n_{cld} = 10^{23}$ m⁻³, respectively [10]. The transverse radius of the cloud $r_{cld} = 3$ mm was determined as described above from the instantaneous photograph of the cloud. The speed of sound $c_s = 1.3 \times 10^4$ m/s was obtained under the assumption of single ionization of hydrogen and carbon. Condition (6) will be satisfied at $M_{cld} = 0.6$. Thus, in further estimates of the density of pellet clouds and the ionization lengths of C^+ ions, it is reasonable to vary M_{cld} in the range of $0.5–1.0$.

Estimates from Eq. (6) are in reasonable agreement with the longitudinal distribution of heavy particles calculated with the parameters of the cloud and the ablation rate at the injection of the carbon pellet into W7-AS discharge no. 43004 reported in [7]. Formula (6) was used to calculate the dependence of the electron density n_{cld} on the temperature T_{cld} at $M_{cld} = 0.5$ and 1 for data of W7-AS discharge no. 43580 presented in Table 1.

The dependences of the measured characteristic longitudinal decay length l_{dec} of the CII line intensity on the suggested electron temperature in the cloud T_{cld} are shown in Fig. 4 for (a) the carbon cloud at the
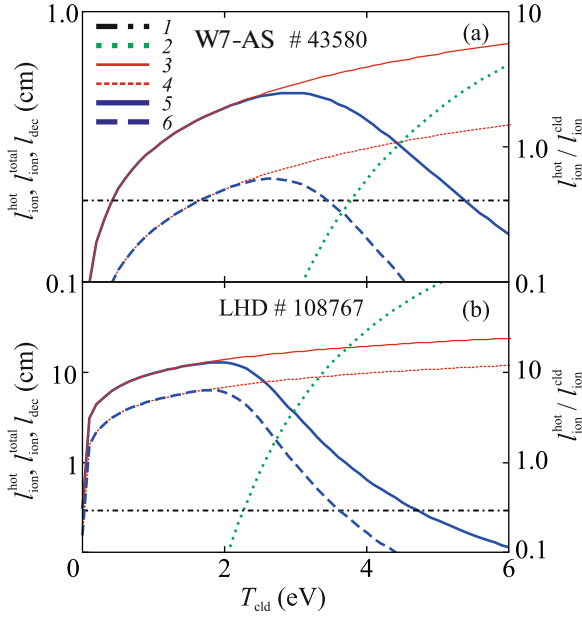
Fig. 4. (Color online) Characteristic lengths (*1*) l_{dec}, (*2*) $l_{ion}^{hot}/l_{ion}^{cld}$, (*3*) $l_{ion}^{hot(M=1)}$, (*4*) $l_{ion}^{hot(M=0.5)}$, (*5*) $l_{ion}^{total(M=1)}$, and (*6*) $l_{ion}^{total(M=0.5)}$ versus the temperature of the pellet cloud.

W7-AS and (b) the hydrocarbon cloud at the LHD in comparison with the dependences of the lengths of electron-impact ionization of C^+ ions in the ground state calculated using Eqs. (5) and (6). The ionization lengths of C^+ ions by hot electrons of the background plasma calculated with $M_{cld} = 1$ and 0.5 are denoted as $l_{ion}^{hot(M=1)}$ and $l_{ion}^{hot(M=0.5)}$, respectively. The lengths of ionization of C^+ ions by hot electrons of the background plasma and cold electrons of the cloud obtained with $M_{cld} = 1$ and 0.5 are denoted as $l_{ion}^{total(M=1)}$ and $l_{ion}^{total(M=0.5)}$, respectively. The dotted line is the ratio $l_{ion}^{hot}/l_{ion}^{cld}$ of the lengths of ionization of C^+ ions by hot and cold electrons, which demonstrates which particles make a larger contribution to ionization.

The behavior of the $l_{ion}^{total(M=1)}$ and $l_{ion}^{total(M=0.5)}$ curves is determined by two competing processes: (i) an increase in the expansion rate with increasing temperature of the cloud and (ii) a rapid, nearly exponential, increase in the rate of ionization by electrons of the cloud with an increase in their temperature. It is seen in Fig. 4a that $l_{ion}^{total(M=1)}$ (line *5*) is smaller than l_{dec} (straight line *1*) in two regions $T_{cld} \leq 0.5$ eV and $T_{cld} \geq 5.5$ eV. The contribution from only hot electrons to the ionization of C^+ ions near $T_{cld} \approx 0.5$ eV corresponding to a low expansion rate is enough to ensure the observed longitudinal decay length of the intensity. However, at such low expansion rates, the electron

density estimated by Eq. (6) is a factor of 3−4 higher than that at a temperature of 5.5 eV corresponding to the second crossing of line *5* with straight line *1*. According to [11], the decrease in the heat flux of hot electrons at such a high density would be stronger than the "experimental" decrease calculated from the measured ablation rate and the parameters of the background plasma. Furthermore, the temperature $T_{cld} \approx 0.5$ eV is noticeably lower than the value obtained in the simulation including the energy balance in the cloud [7]. Consequently, the more realistic temperature is $T_{cld} \approx 5.5$ eV that corresponds to the second crossing and at which the contribution of electrons of the cloud to ionization becomes noticeable. The total contribution from hot and cold electrons to ionization is sufficient to ensure the observed longitudinal decay length of the CII line intensity upon expansion at the speed of sound occurring at a temperature of 5.5 eV. In this case, the rate of cold-electron ionization will be a factor of 2.5 higher than the rate of hot-electron ionization (see line *2* in Fig. 4a). To explain the experimentally observed longitudinal decay length of the CII line intensity in the case of subsonic expansion at $M_{cld} = 0.5$, a smaller contribution from cold electrons of the cloud to the ionization of C^+ ions is required and a temperature of $T_{cld} \approx 3.5$ eV is sufficient, which is lower than that in the case of expansion at the speed of sound. The corresponding rate of hot-electron ionization will be a factor of 6 higher than the rate of cold-electron ionization.

Temperatures of 3.5−5.5 eV evaluated by the above method are in agreement with temperatures of 2.5−5.0 eV previously obtained in the simulation in the region of the cloud, where the intense ionization of C^+ ions occurs [7].

As seen in Fig. 4b for the hydrocarbon cloud at LHD, the contribution to ionization from hot electrons of the background plasma is much smaller than the contribution of electrons of the cloud at any supposed regime of expansion of the ablatant because of a much stronger decrease in the flux of hot electrons (by a factor of more than 5 compared to the case of carbon clouds). A temperature of 3.5−4.5 eV is sufficient in this case to ensure the observed decay length of the CII line intensity. The presented values are also in agreement with the measurements of the temperature in the hydrocarbon cloud [9, 10].

4. CONCLUSIONS

To summarize, the measured dimensions of pellet clouds emitting the CII line, as well as the calculated electron temperature and density in a cloud, have been analyzed. It has been shown that the contribution of hot electrons of the discharge plasma is insufficient to reproduce the experimentally observed longitudinal decay lengths of the CII line intensity. It is necessary

to take into account the ionization of C^+ ions by cold electrons of the cloud. This process is particularly important in hydrocarbon clouds, where cold electrons of the cloud make the leading contribution to ionization because electron flux from the hot plasma is strongly shielded. This contribution is more than an order of magnitude larger than that from hot electrons of the discharge plasma. Hot and cold electrons in carbon clouds make close contributions to ionization. The contributions from cold and hot electrons can prevail in the cases of expansion at the speed of ion sound and at subsonic velocity, respectively. The analysis of experimental data on the parameters of hydrocarbon clouds shows that the velocity of expansion can differ from the speed of sound by a factor of about 0.5. Experimental data for carbon clouds are insufficient for a reliable conclusion on the character of expansion.

FUNDING

CONFLICT OF INTEREST

The authors declare that they have no conflicts of interest.

OPEN ACCESS

REFERENCES

1. B. V. Kuteev, Tech. Phys. **44**, 1058 (1999).

2. B. Pégourié, Plasma Phys. Control. Fusion **49**, R87 (2007).

3. L. L. Lengyel, Nucl. Fusion **29**, 325 (1989).

4. P. R. Goncharov, T. Ozaki, S. Sudo, N. Tamura, TESPEL Group, LHD Experimental Group, E. A. Veshchev, V. Y. Sergeev, and A. V. Krasilnikov, Rev. Sci. Instrum. **77**, 10F119 (2006).

5. O. A. Bakhareva, V. Y. Sergeev, B. V. Kuteev, V. G. Skokov, V. M. Timokhin, R. Burhenn, and W7-AS Team, Plasma Phys. Rep. **31**, 282 (2005).

6. K. L. Bell, H. B. Gilbody, J. G. Hughes, A. E. Kingston, and F. J. Smith, J. Phys. Chem. Ref. Data **12**, 891 (1983).

7. D. K. Morozov, V. Gervids, I. Y. Senichenkov, I. Y. Veselova, V. Rozhansky, and R. Schneider, Nucl. Fusion **44**, 252 (2004).

8. I. A. Sharov, V. Y. Sergeev, I. V. Miroshnikov, N. Tamura, B. V. Kuteev, and S. Sudo, Rev. Sci. Instrum. **86**, 043505 (2015).

9. I. A. Sharov, V. Y. Sergeev, I. V. Miroshnikov, B. V. Kuteev, N. Tamura, and S. Sudo, Tech. Phys. Lett. **44**, 384 (2018).

10. I. A. Sharov, V. Yu. Sergeev, I. V. Miroshnikov, N. Tamura, and S. Sudo, Plasma Phys. Control. Fusion **63**, 065002 (2021).

11. B. V. Kuteev, V. Yu. Sergeev, and L. D. Tsendin, Sov. J. Plasma Phys. **10**, 675 (1984).

12. S. J. Blanksby and G. B. Ellison, Acc. Chem. Res. **36**, 255 (2003).

13. V. Yu. Sergeev, O. A. Bakhareva, B. V. Kuteev, and M. Tendler, Plasma Phys. Rep. **32**, 363 (2006).

14. B. V. Kuteev, Nucl. Fusion **35**, 431 (1995).

15. V. A. Rozhansky and I. Y. Senichenkov, Plasma Phys. Rep. **31**, 993 (2005).

16. L. Ledl, R. Burhenn, L. Lengyel, F. Wagner, V. Y. Sergeev, V. M. Timokhin, B. V. Kuteev, V. G. Skokov, and S. M. Egorov, Nucl. Fusion **44**, 600 (2004).

17. V. Rozhansky, Phys. Plasmas **20**, 101614 (2013).

Translated by R. Tyapaev